Heliyon 10 (2024) e33448

Contents lists available at ScienceDirect

Heliyon

journal homepage: www.cell.com/heliyon

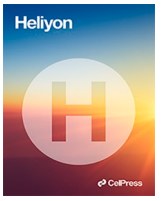

Research article

Modeling the impacts of extreme climate scenarios on soil acidity (pH and exchangeable aluminum) in Abbay River Basin, Ethiopia

Fedhasa Benti Chalchissa [a,*], Birhanu Kebede Kuris [b]

[a] Center for Energy and Environmental Research, Wollega University, Ethiopia
[b] Environmental Science Program, Department of Biology, Ambo University, Ethiopia

ARTICLE INFO

Keywords:
Abbay river basin
Artificial neural network
Climate factors
Soil acidity
Model validation

ABSTRACT

The Abbay River Basin faces the looming threat of extreme climate events, including prolonged droughts and erratic rainfall patterns, which can significantly affect soil health and fertility. This study aimed to explore the influence of extreme climate conditions on soil pH and exchangeable aluminum, aiming to promote sustainable agricultural practices in Ethiopia. The Africa Soil Information Service (ASIS) provided datasets on soil pH and exchangeable aluminum. The European Copernicus Climate Change Data Store was used to download historical and future datasets of extreme climatic indices from 1980 to 2010 and 2015–2050, respectively. The Coupled Model Intercomparison Project Phase 6 model ensemble was used to predict future climate impacts under three shared socioeconomic scenarios: SSP1-2.6, SSP2-4.3, and SSP5-8.5. Data extraction, quality control, and clustering were conducted before analysis, and the model was validated for its accuracy and reliability in predicting soil parameter changes. An artificial neural network model was utilized to predict the effects of extreme climate indices on soil pH and exchangeable aluminum concentrations. The model was designed to accurately and reliably predict changes in soil parameters. This study compared the changes in soil pH and aluminum concentrations using paired t tests. The model's diagnostic results indicated a significant impact of extreme climate scenarios on soil pH and exchangeable aluminum. Extreme climate factors such as heavy precipitation and cooler night time temperatures significantly contribute to soil acidification and an increase in aluminum concentration. Under the SSP1-2.6 and SSP2-4.5 emission scenarios, soil pH levels are expected to increase by 8.38 % and 3.79 %, respectively. These changes in soil pH are expected to have significant impacts on the exchangeable aluminum content in the soil, with increases of 37 % and 5.38 %, respectively, under the same emission scenarios. However, the SSP5.8 scenario predicted a 45 % increase in exchangeable aluminum and a 9.36 % decrease in soil pH. Therefore, this study significantly enhances our understanding of the influence of climate change on soil health. The development of strategies to mitigate climate change impacts on agriculture in the region must consider the effects of extreme climate indices.

1. Introduction

The Abbay River Basin, located in Ethiopia, is critical for the country's agricultural productivity and water resources. However, the region faces the threat of extreme climate events, including prolonged droughts and erratic rainfall patterns, which can significantly

* Corresponding author.
E-mail address: fedeesa@gmail.com (F. Benti Chalchissa).

https://doi.org/10.1016/j.heliyon.2024.e33448
Received 9 June 2023; Received in revised form 21 June 2024; Accepted 21 June 2024
Available online 22 June 2024

impact soil health and fertility [1]. Among the key indicators of soil health are pH and exchangeable aluminum concentration, both of which play vital roles in determining soil productivity and crop yield. The concentration of hydrogen ions in the soil determines the pH, which represents the acidity or alkalinity of the soil solution [2,3]. It influences the availability of essential nutrients to plants, as well as the activity of microorganisms that play a crucial role in soil fertility. The pH of the soil affects the availability of essential nutrients, such as nitrogen, phosphorus, and potassium, to plants [4–6]. On the other hand, exchangeable aluminum refers to the amount of aluminum ions available for plant uptake, but high levels of Al^{3+} can be toxic to plants, causing stunted growth, reduced yields, and even death [7]. Therefore, understanding the relationship between soil pH and exchangeable aluminum is crucial for farmers and gardeners to ensure optimal plant growth and yield.

Extreme climatic indicators and soil acidity are important factors to consider when studying the effects of climate change on soil properties. Climatic factors such as temperature and precipitation patterns can affect the physiochemical properties of soils [8]. Soil properties such as nutrient availability, pH, and moisture content can also influence ecosystem dynamics by affecting plant growth and nutrient cycling. Understanding these relationships is crucial for predicting how soils in ecosystems will respond to future climate change scenarios [8]. Several factors affect soil pH and exchangeable aluminum levels, including soil type, climate, vegetation, and human activities such as fertilization and irrigation [9]. In areas with high rainfall, leaching can occur, where water percolating through the soil can dissolve and carry away basic cations (such as calcium, magnesium, and potassium) from the soil, leading to the accumulation of acidic ions (such as hydrogen and aluminum) and resulting in acidic soils. Conversely, in arid or semiarid regions with low rainfall and limited leaching, basic cations may accumulate in the soil over time, leading to alkaline soils. The type of vegetation in an area can also affect soil pH, as some plants release acidic compounds into the soil [10], while others release alkaline compounds. Additionally, human activities such as the use of fertilizers and irrigation can also impact soil pH and exchangeable aluminum levels [11]. Extreme climate scenarios such as drought, flooding, and increased temperatures can have significant impacts on soil pH and exchangeable aluminum levels [12,13]. For example, heavy rainfall can lead to the leaching of nutrients and increase soil acidity, while drought can cause the accumulation of salts and increase soil alkalinity. Flooding can also lead to an increase in soil pH due to the decomposition of organic matter, which releases alkaline compounds [12,14].

Extreme temperatures, both hot and cold, can also affect these levels due to changes in microbial activity and nutrient availability and thus can alter soil pH [15–17]. These factors must be considered when managing soil conditions for optimal plant growth and yield under changing climate conditions. These scenarios can have negative impacts on crop production and highlight the need for proper management practices to mitigate their effects. Although vegetation and human activities can affect soil pH and aluminum levels, extreme climate scenarios can have a much greater impact that cannot be controlled by farmers and gardeners.

Previous research on climate change and soil chemistry has shown that increasing temperatures and increased precipitation can lead to changes in soil chemistry, such as increased acidity and aluminum toxicity [17–19]. This can have negative impacts on crop growth and yield, as well as on soil health and fertility. However, there is also evidence that certain management practices, such as using cover crops and reducing tillage, can help mitigate the effects of extreme weather events on soil pH and exchangeable aluminum [20,21]. Overall, the literature highlights the importance of proactive soil management in the face of changing climate conditions. However, there are several examples where extensive management practices may not be sufficient to counter the negative impacts of climate change on soil pH and exchangeable aluminum. For instance, a study conducted in Ethiopia revealed that prolonged droughts associated with climate change led to severe soil degradation, including high levels of soil acidity and exchangeable aluminum, despite farmers' efforts to apply lime and other management practices [22–25].

Although there is a significant amount of research on climate change and soil chemistry, there are still gaps in our understanding of the complex relationships between these factors. Therefore, detailed research is essential to fully understand the complex association between climate change and soil chemistry [8,26–28]. The Abbay River Basin in Ethiopia is an important agricultural area, with much of the region's economy relying on the productivity of its soils. However, the basin is facing various challenges, such as heavy precipitation (flooding), drought, deforestation, soil acidity, erosion, and soil toxicity, which threaten the sustainability and well-being of local communities [29–31] and can significantly impact the soil pH and exchangeable aluminum levels [29,32]. The soil acidity problem in this river basin is obvious due to high levels of extreme rainfall and temperature variability. In this region, the annual rainfall and surface temperature are highly variable and often result in soil erosion, which can further exacerbate the alteration of soil pH and release exchangeable aluminum from its parent matter [33–35].

Moreover, a limited number of earlier studies were based on the impacts of temperature and rainfall changes on soil health using Coupled Model Intercomparison Project phases 3 (CMIP3) and 5 (CMIP5) emission scenarios [16,18,36,37]. These scenarios, which included only a limited range of possible future emissions, may not accurately reflect the current state of climate change impacts on soil quality [38]. However, the novelty of this study lies in its focus on the effects of extreme climate scenarios on soil pH and exchangeable aluminum in the Abbay River Basin using the most recent model (CMIP6). The latest model offers more precise predictions for future climate change effects on soil properties by considering a wider range of emission scenarios. The CMIP6 scenarios consider feedback mechanisms and other factors that were not included in previous models, making them more comprehensive tools for understanding the complex dynamics of climate change on soil health [39,40]. This study employed multiple regression, bootstrapped forest, and neural network models to analyze our data. Multiple regression is a widely used statistical technique that models the relationship between a dependent variable and multiple independent variables. It is chosen for its interpretability and ease of implementation [40]. The bootstrapped forest model, an ensemble learning method, combines multiple decision trees to improve the predictive accuracy and reduce overfitting [41]. This model is selected for its robustness and ability to handle complex, nonlinear relationships in the data. Neural networks, inspired by the human brain, consist of interconnected layers of nodes that can learn patterns and make predictions. They are included in this study because of their powerful ability to capture intricate patterns and dependencies within the data [42]. These models were chosen to provide a comprehensive comparison of traditional, ensemble, and advanced machine learning

techniques, allowing us to evaluate their performance and suitability for our specific research objectives.

Therefore, understanding the potential interactive effects of extreme climate scenarios on soil pH and exchangeable aluminum using the most accurate model is crucial for effective land management and agricultural sustainability in the Abbay River Basin. This requires a comprehensive modeling approach that integrates climatic data, soil properties, and land management practices to forecast potential changes and inform adaptation strategies. This study aims to address this gap by employing advanced modeling techniques to simulate the impacts of extreme climate scenarios on soil pH and exchangeable aluminum concentrations in the Abbay River Basin. By combining climate projections with soil data and land management practices, we seek to elucidate the complex interactions between climate change and soil properties. This paper provides an introduction to the climate and soil pH literature, explains the research methodology, presents findings, and discusses implications for advancing soil science and climate change studies.

2. Methodology

2.1. Study location

The study was conducted in the Abbay River Basin in the highlands of Ethiopia. It is one of the major river basins in Ethiopia; it is located between 7°45′ and 12°45 N and 34°05′ and 39° 45' E, and it covers an area of 199,812 km^2, with a total perimeter of 2,862 km (Fig. 1). The basin is home to a diverse range of flora and fauna, which are very important for the ecological balance of the region [43]. The Abbay River basin is also a crucial source of water for agriculture and hydropower generation, supporting the livelihoods of millions of people in Ethiopia and downstream countries such as Sudan and Egypt [30]. The climate of the Abbay River basin is characterized by three distinct seasons: short rainy seasons from February to May, a dry season from October to January (Bona), and a rainy season from June to September [43,44]. It ranges from semiarid deserts in the lowlands to humid and warm (temperate) conditions in the southwest and is dominated by altitudes ranging from 526 m to 3904 m [45]. This characteristic determines the local climate, which ranges from dry-hot to cool-moist, with the mean temperature of the warmest month above 18 °C to temperate on the high plateau and cold on the mountain peaks, with the mean temperature in the coldest month below 10 °C. The annual rainfall varies between approximately 800 mm and 2,220 mm, with a mean of approximately 1,420 mm [46]. The climate in this region is influenced by the monsoon season, which brings heavy rainfall from June to September [47]. The vegetation in this area includes tropical rainforests, deciduous forests, and alpine meadows [43].

2.2. Data collection

2.2.1. Soil data

Soil pH and exchangeable aluminum (Al^{3+}) datasets at 0–20 cm depths were downloaded from the African Soil Information Service (ASIS). Since 2008, the International Soil Reference and Information Centre (ISRIC) has provided soil pH and exchangeable aluminum for ASIS datasets through an online data portal on the ISRIC website, where users can freely access a wide range of soil-related information and tools that can be used for research, policy-making, and land management purposes [48] at https://data.isric.org/geonetwork/srv/eng/catalog.search#/home The ASIS has emerged as a leading African authority on soil science, significantly advancing public understanding of soil resources through research and outreach. The ISRIC was also established in 1966 to provide

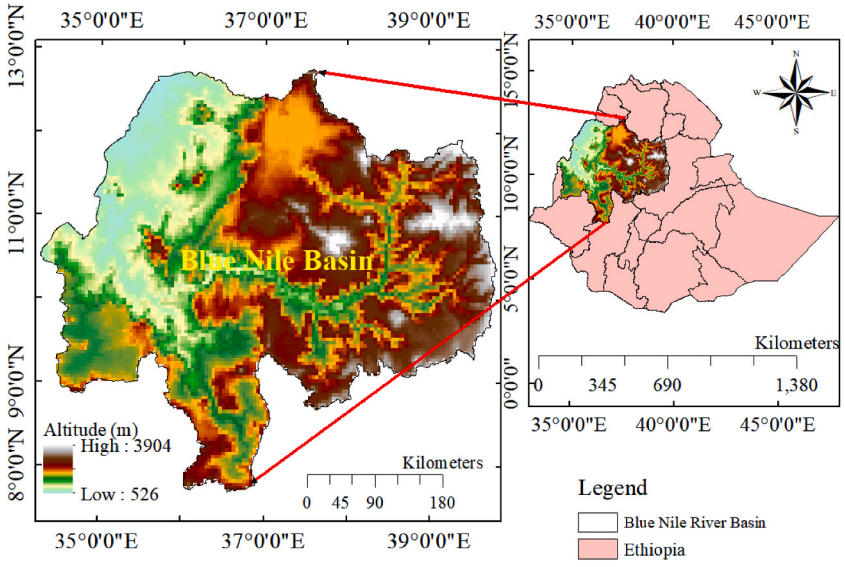

Fig. 1. Location maps of the study area.

reliable, standardized soil information for sustainable land use planning and management, promoting international cooperation in soil research and education [49].

2.2.2. Climate data

The extreme climate datasets were obtained from the European Copernicus Climate Data Store (C3S), a platform offering free and open access to climate data on the European Union's website (https://cds.climate.copernicus.eu/cdsapp#!/home). CMIP6 offers 27 GCMs for the global simulation of current and future extreme climate indicators. However, the study utilized only five climate models, CNRM-CM6-1, CNRM-CM6-1-HR, CNRM-ESM2-1, MIROC-ES2L, and UKESM1-0-LL, to analyze the effects of extreme climate indicators on soil pH and exchangeable aluminum based on the availability of data at this particular site. This tool aids in climate change adaptation and mitigation by providing updated and accurate data on climate factors such as temperature and precipitation extremes [50]. The platform provides data analysis and visualization tools, making it a valuable resource for researchers, policymakers, and the general public and allowing access to various sources [51]. These data portals are excellent data resources for climate change research, providing highly dependable ETCCDI data [39,50,52], suggesting that these data can be utilized to analyze climate patterns and trends and to create models for predicting future climate change impacts. This study used three shared socioeconomic pathways—SSP1-2.6, SSP2-4.5, and SSP5-8.5—from the Coupled Model Intercomparison Project Phase 6 (CMIP6) to accurately predict past and future climates, as per the IPCC's sixth assessment report. Based on the Pearson correlation coefficient values, six extreme climatic indicators were selected for analysis. These indicators are heavy precipitation days (R95P), extremely heavy precipitation days (R99P), cold nights (TN10P), warm nights (TN90P), cold days (TX10P), and warm days (TX90P). The selected indicators are presented in Table 1.

2.3. Data preparation and screening

Data extraction: The climate and soil datasets were obtained using ArcMap, which was then filtered from GeoTIFF and NetCDF file formats at a resolution of 0.04° from the same sample points. This resolution is commonly used for global or regional analyses and modeling [53]. These datasets can provide valuable information for various applications, such as agriculture, forestry, hydrology, and climate change studies [49]. However, the accuracy and reliability of datasets are influenced by the quality of the input data and the methods used for processing and analysis. Therefore, these data underwent processing and quality control checks to ensure accuracy and consistency before being used for analysis.

Multicollinearity test: The analysis considered the multicollinearity of climatic variables to identify dependencies. Through the calculation of variance inflation factors (VIFs) for each variable, where a VIF value above 10 indicates high multicollinearity and a value lower than 10 indicates low multicollinearity. The results revealed that certain climatic variables, including very heavy precipitation (R95P), extremely heavy precipitation (R99P), cold nights (TN10P), warm nights (TN90P), cold days (TX10P), and warm days (TX90P), had VIF values below 10, indicating no significant multicollinearity. This approach helped ensure that the results obtained were not biased by multicollinearity [54].

Outliers test: Outliers were identified and removed from datasets using statistical methods called the interquartile range (IQR). The "normal" range of data in this method is defined as values between the first quartile (Q1) and the third quartile (Q3). Statistically significant outliers were identified as data points that fell outside a specific range of values. The method is robust to extreme values and nonnormal distributions, ensuring reliable and representative data for analysis in the study area [55]. However, removing outliers can significantly impact statistical analysis results and lead to inaccurate conclusions [55], so careful consideration was given to the overall interpretation of the data.

Data clustering: Data clustering is a statistical technique that groups similar data points based on their shared characteristics or attributes [56,57]. The K-means clustering algorithm was used to cluster the historical dataset, assigning data points based on their proximity to the cluster centroid [58]. This technique is used to identify patterns and relationships within large datasets, facilitating data analysis and machine learning [56]. It simplifies complex datasets by grouping similar data points together, revealing insights that may not be immediately apparent. The process typically involves assessing the homogeneity of the data by comparing the similarities between each data point and arranging them accordingly [59,60]. The homogeneity of each dataset was assessed through statistical tests using Tukey's honestly significant difference test. The analysis focused on determining significant differences between groups based on the mean values of soil pH. Compared with the other clusters, the third cluster had significantly lower soil pH values, indicating heavy precipitation and extremely heavy precipitation at the $P = 0.01$ significance level (Table 2).

'In this study, the clustered datasets were analyzed to identify any spatial trends or patterns (Fig. 2a). The mapping of these datasets, as illustrated in the provided text, allowed us to visually interpret the distribution and relationships within the data. K-means

Table 1
Selected extreme climatic indictors.

Code	Indicators	Description s	Unit
R95P	Very heavy rainfall	Annual total rainfall when RR > 95th percentile	mm
R99P	Extremely heavy rainfall	Annual total rainfall when RR > 99th percentile	mm
TN10P	Cool nights	Days when daily minimum temperature <10th percentile	Day
TN90P	Warm nights	Days when daily minimum temperature >90th percentile	Day
TX10P	Cool days	Days when daily minimum temperature <10th percentile	Day
TX90P	Warm days	Days when daily minimum temperature >90th percentile	Day

clustering is a powerful and widely used technique for data clustering (Fig. 3b). This approach aids in identifying hidden patterns, simplifying data analysis, and making informed decisions across various domains while also enhancing dataset comprehension [61]. Moreover, this approach aids in identifying outliers and enhancing the overall comprehension of the data [62]. Overall, data clustering is a crucial technique for analyzing large datasets and gaining valuable insights [61,62]. The identification of low, medium, and high rates of soil acidity allowed for the implementation of targeted interventions.

2.4. Data analysis

2.4.1. Model validation and selection

Model validation and selection are critical steps in the machine learning process. This study utilized cross-validation techniques to validate and select the most effective model for predicting soil acidity. K-fold cross-validation is a technique used to ensure the robustness of a model's performance on small datasets. K-fold cross-validation involves dividing the data into 3 subsets—training (70 %), validation (15 %), and testing (15 %)—and modeling three times—using different subsets for each training, validation, and testing. The distribution was chosen to ensure the model's accuracy in assessing the performance on both known and unseen data. The training data allowed the model to learn the patterns and relationships within the dataset, while the validation data helped fine-tune the hyperparameters and prevent overfitting. Finally, the testing data provided a final evaluation of the model's performance before deployment. The neural network model was selected based on its performance on fresh data using R-squared (R^2), the root mean square error (RMSE), and the absolute mean error (AAE). The method ensures the model's accuracy in predicting its performance on future data without overfitting or under fitting it [63]. Machine learning and predictive modeling aim to make accurate predictions about future data, with comparative analysis identifying the best-performing model for specific datasets.

The validation analysis revealed that the artificial neural network was the most accurate model for predicting soil pH and the Al^{3+} concentration. The artificial neural network showed higher R^2 values than did the multiple regression and bootstrapped forest models, while the RMSE and AAE ANN models had lower R^2 values for the soil pH and exchangeable aluminum datasets (Table 3). A higher R^2 value indicated that the model was accurate and reliable, while the R^2 values of the RMSE and AAE were lower.

Fig. 3 shows a 1:1 fit line in a plot comparing the actual and predicted values of the three different models. The multiple regression and bootstrapped forest models exhibited higher error levels than did the ANN model, indicating a lack of improved data alignment. Therefore, the superior accuracy of the ANN model is attributed to its ability to recognize complex nonlinear relationships between climate and soil pH datasets in both training and validation plots (Fig. 3a and b). Similarly, the ANN model successfully captured the relationship between datasets of extreme climate indicator and soil Al^{3+} levels, demonstrating strong correlations in both training and validation plots (Fig. 3 c and d). The ANN model's multiple layers of neurons may enable it to detect subtler data patterns than other models, according to Refs. [64,65]. The model's accuracy and usefulness in predicting soil properties under changing climatic conditions require continuous monitoring and refinement. However, the model's performance may differ when applied to additional data. The models' accuracy was assessed using new soil and future extreme climate datasets to ensure reliability and generalizability, but their data were not included in the manuscript.

2.4.2. Model performance evaluation

After training a model on a dataset, it is important to evaluate its performance on new data to ensure that it is not overfitting or under fitting. According to Ref. [66], the number of neurons in a model significantly influences the accuracy and efficiency of the model. Under fitting occurs when a model's neuron is too small and unable to capture complex data patterns, and overfitting occurs when the model neuron becomes too large and memorizes noise instead of learning meaningful patterns [64]. The trial-and-error method is crucial for achieving optimal performance by finding the appropriate balance of neurons. Table 4 shows trial-and-error methods for analyzing various neurons. The study revealed that ten neurons in both the training and testing sets exhibited increased generalized R^2 values and decreased negative log likelihood values. Therefore, the model's suitability for the data was confirmed by a higher R^2 value and a lower negative log likelihood value.

Therefore, a neural network model was utilized to predict the interaction effects of various climatic extremes on soil pH and exchangeable aluminum.

Model Transferability: Model transferability refers to a machine learning model's ability to perform effectively on a related task after being trained on one task. This study assessed neural network model transferability using statistical metrics such as generalized R2 and negative log likelihoods for source tasks and targeted task datasets. The source task focused on predicting the impacts of extreme climate indicators on soil acidity, while the target task was to predict the effects of rainfall and temperature on the organic carbon dynamics of the soil, which have different objectives or labels of interest. A baseline model was trained using data from the target task, and the R^2 (coefficient of determination) and negative log likelihood were computed for this model. Table 5 reveals

Table 2
K-mean values of the soil and climate parameters under each cluster.

Cluster	Soil pH	Al^{+3}	R95P	R99P	TN10P	TN90P	TX10P	TX90P
1	6.52^{c}	0.09^{b}	68.78^{b}	14.57^{c}	34.14^{a}	1.76^{b}	35.59^{a}	0.67^{b}
2	6.23^{b}	0.15^{b}	86.21^{ab}	34.57^{b}	31.14^{a}	3.63^{b}	32.39^{a}	1.08^{b}
3	5.44^{a}	0.34^{a}	117.13^{a}	42.63^{a}	23.14^{b}	1.21^{a}	25.31^{b}	2.51^{a}

Note that the mean values of variables in the same column with the same letter indicate no significant difference between the datasets in the cluster.

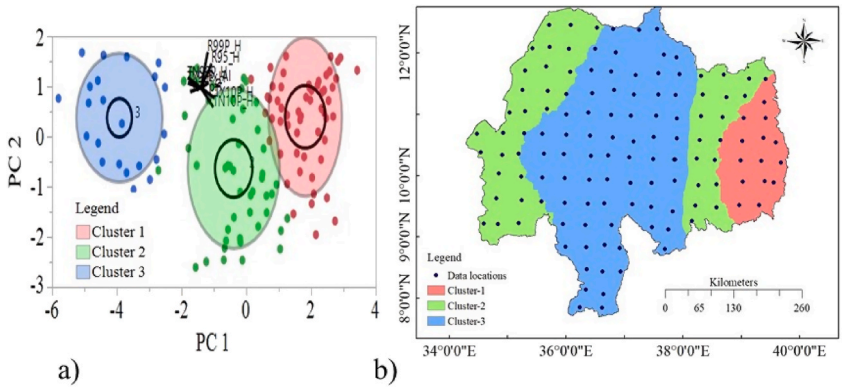

Fig. 2. Dataset clustering based on the means of the variables (a) and mapping (b).

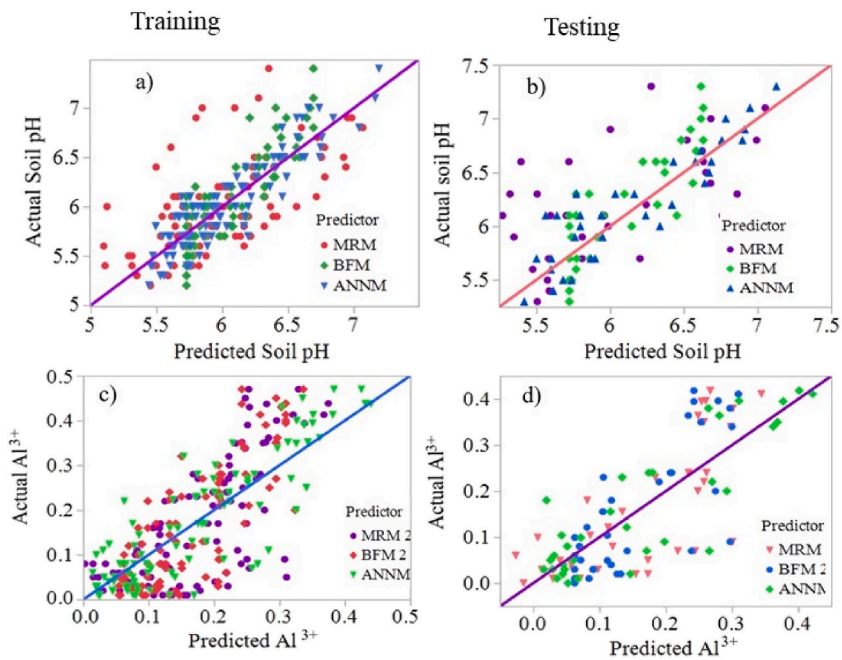

Fig. 3. Analysis of the 1:1 fit line using actual and predicted datasets for soil pH and Al^{3+} in training (a and c) and testing (b and d).

Table 3
Comparative analyses of model performances for selection using model parameters.

Soil Variables	Models	Training			Validation		
		R^2	RMSE	AAE	R^2	RMSE	AAE
Soil pH	Multiple Regression	0.27	0.40	0.30	0.09	0.53	0.41
	Bootstrapped Forest	0.71	0.25	0.20	0.65	0.30	0.26
	Artificial Neural Network	**0.82**	**0.20**	**0.17**	**0.80**	**0.23**	**0.19**
Al^{3+}	Multiple Regression	0.50	0.10	0.08	0.56	0.09	0.07
	Bootstrapped Forest	0.61	0.09	0.07	0.58	0.09	0.08
	Artificial Neural Network	**0.74**	**0.07**	**0.05**	**0.74**	**0.07**	**0.06**

The bolded predictive model and its parameter values are the most accurate and reliable models chosen for this study.

significant variation in the statistical metrics and measures across different levels of neurons, as evident from the analysis. The R^2 values for training and testing indicate varying accuracy levels, with higher numbers indicating superior performance at ten neurons. Additionally, the negative log likelihood values at neuron 10 provide insight into the model's fit to the data, with lower values suggesting a better fit. The negative log likelihood values indicate the level of model performance, with lower values indicating better

Table 4
Evaluation of the ANN model's predictive performance.

No of Neuron	Training		Testing	
	Generalized R^2	-Log likelihood	Generalized R^2	-Log likelihood
3	0.95	−136.98	0.96	−47.70
5	0.96	−152.87	0.96	−49.76
10	**0.98**	**−158.34**	**0.97**	**−50.56**
15	0.97	−157.18	0.96	−47.50

Note: The bolded numbers indicate the optimal number of neurons for optimal predictive model performance.

Table 5
Measuring the statistical metrics of the transfer model for different levels of neurons.

No of Neuron	Training		Testing	
	Transfer R^2	Transfer -Log likelihood	Transfer R^2	Transfer -Log likelihood
3	0.93	−126.05	0.91	−45.20
5	0.91	−143.69	0.92	−47.40
10	**0.98**	**−168.12**	**0.90**	**−50.46**
15	0.94	−147.61	0.81	−39.87

performance and higher values indicating poorer performance [67]. Overall, these metrics highlight the importance of selecting the appropriate number of neurons to achieve optimal results in neural network modeling.

The R^2 transfer index was calculated using equation (1) to measure the proportion of variance explained by a transferred model in a target task compared to a baseline model.

$$TI = \frac{TR^2}{R^2} \tag{1}$$

where TI is the transfer index, TR^2 is the transfer coefficient of determination, and R2 is the baseline coefficient of determination.

The model's relative performance difference was evaluated using negative log likelihood, resulting in more precise performance. Relative model transferability was calculated by comparing the absolute or relative performance difference between the source and target tasks using simple equation (2).

$$\mathrm{RTE}\% = \left(\frac{-Log\ likelihood_t - (-Log\ likelihood_b}{-Log\ likelihood_b}\right) * 100 \tag{2}$$

where RTE is the relative model transferability, -log likelihood is the model accuracy on the targeted task, and -log likelihood is the model accuracy on the source task.

Table 6 clearly shows that there is a significant variation in the transfer indices as the number of neurons trained increases. A tenth of trained neurons lead to higher transfer indices, indicating better performance in transferring knowledge from one task to another. The relative negative log likelihood also increases with the number of tenth trained neurons. Overall, these results highlight the importance of considering the number of neurons trained when assessing model transferability.

After model training using historical extreme climate data, the relative changes in soil pH and exchangeable aluminum levels at the same locations were calculated. The method presented in Ref. [68] was used to calculate changes in soil parameters as changes in extreme climate indicators using equation (3).

$$\Delta\mathrm{SP}\% = \left(\frac{\mathrm{PSP_i} - \mathrm{HSP_i}}{\mathrm{HSP_i}}\right) * 100 \tag{3}$$

where ΔSP% indicates the percent change in the soil parameters (soil pH and Al^{3+}), PSP is the predicted soil parameter, i is the average soil pH or Al^{3+}, and HSP is the historical value of the soil parameter.

Table 6
Neural network model transferability analysis.

Neuron	Training	
	Transfer Indices	Relative error (%)
3	0.98	6.21
5	0.95	21.07
10	**0.99**	**5.82**
15	0.97	11.50

3. Results

3.1. Soil pH and exchangeable aluminum estimation under the current and future scenarios

3.1.1. Soil parameters under the historical climate extremes scenario (1981–2010)

Table 7 presents the estimates of the soil pH and exchangeable aluminum (Al^{3+}) parameters under the baseline climate conditions. The NNM diagnostic results indicate that the increase in extreme climate indicators in the Abbay River Basin significantly increased soil acidity ($p < 0.005$). A one-unit increase in R95P, R99P, and TN10P significantly decreased the pH by −0.012, −0.017, and −0.18 for R95P and R99P, respectively, while increasing the Al^{3+} concentration by 0.003, 0.002, and 0.008 mg/kg, respectively.

On the other hand, the present study also revealed that a one-unit increase in TX10P significantly increased the soil pH by 0.375 and decreased the Al^{3+} concentration by −0.012 g/kg, while an increase in TN90P increased the Al^{3+} concentration by 0.086 g/kg. An insignificant increase in TN90P significantly decreased Al^{3+} by −0.062 g/kg of bulk soil ($p = 0.0403$).

3.1.2. Soil pH and exchangeable aluminum estimation under future climate change scenarios (2015–2100)

3.1.2.1. Soil parameter estimation under the SSP2.6 scenario. This study predicts significant changes in soil pH and Al^{3+} levels under the SSPP2.6 scenario from 2015 to 2100, as shown in Table 8. The increases in TN90P, TX10P, and TX90P significantly decreased the soil pH by 0.5, 0.32, and 0.22 units, respectively, but increased with increasing TN10P ($P < 0.05$). On the other hand, under a one-mm increase in R95P, the amount of Al^{3+} ions in the SSP2.6 scenario significantly increased by 0.002 mg/kg. A 1 % increase in TX10P and TX90P decreased the concentration of Al^{3+} ions by 0.08 and 0.07 mg/kg, respectively ($P < 0.05$).

Fig. 4 shows the significant interaction effects between extreme climate indicators on soil pH and Al^{3+} ions. The study estimated soil pH values at 5.85 and 6.34 units under the historical and SSP2.6 scenarios, respectively, based on the normal distribution of predictor variables. The study also predicted Al^{3+} ions to be 10.186 and 0.12 mg/kg for the historical and SSP2.6 scenarios, respectively. However, under extreme climate conditions, the interaction effects of extreme temperature and precipitation events on soil pH and Al^{3+} ions were significant, leading to changes in soil chemistry that could have negative impacts on agricultural productivity.

3.1.2.2. Soil parameter estimation under the SSP4.5 scenario. Table 9 shows how soil pH and Al^{3+} react to extreme climate indicators under the SSP4.5 and SSP8.5 scenarios. This study revealed a significant decrease in soil pH and an increase in the Al^{3+} ion concentration under this scenario. The model indicated that a one-mm increase in R99P significantly lowered the soil pH by 0.03 units but did not significantly increase the Al^{3+} concentration. A 1 % increase in TX10P and TX90P significantly increased the soil pH by 1.3 and 0.38, respectively, but decreased the Al^{3+} ion concentration by 0.10 g and 0.01 g/kg, respectively.

Fig. 5 also illustrates the impact of extreme climate indicators on soil pH and Al^{3+} in the SSP4.5 and SSP8.5 scenarios. The soil pH and Al^{3+} ion concentration were within acceptable ranges for the SSP4.5 and SSP8.5 scenarios, with normal predictor values of 6.09 and 5.28 units, respectively, and the Al^{3+} ion concentration was also estimated to be 0.18 and 0.24 mg/kg for the SSP4.5 and SSP8.5 scenarios, respectively. The SSP4.5 and SSP8.5 scenarios predicted that increased R95P and TN10P would decrease soil pH levels and increase Al^{3+} ion concentrations.

3.1.2.3. Soil parameter estimation under the SSP8.5 scenario. Table 10 presents a comprehensive analysis of soil pH and Al^{3+} ion estimation under the SSP8.5 climate change scenario. Under the SSP8.5 scenario, the soil pH is predicted to decrease, while the concentration of Al^{3+} ions is expected to increase significantly. The most significant predictors that reduce soil pH are R95P, R99P, and TX90P, with an increase in these predictors causing a significant decrease in soil pH. The most important predictors that notably reduced soil pH under this scenario were R95P, R99P, and TX90P, indicating that as the number of predictors increased by one unit, the soil pH considerably decreased by 0.018, 0.031, and 0.186 units, respectively. On the other hand, the predictor TN90P is expected to positively affect soil pH, potentially increasing it by 0.063 ($P = 0.007$) with an increase of one percent. The concentration of

Table 7
Estimated soil parameters under historical extreme climate indicators.

Predictors	Responses	Estimates	Std Error	t Ratio	Sign
R95P	Soil pH	−0.012	0.004	−3.28	0.0015
	Al^{3+}	0.003	0.001	4.19	0.0001
R99P	Soil pH	−0.017	0.004	−4.55	0.0001
	Al^{3+}	0.002	0.001	2.35	0.0001
TN10P	Soil pH	−0.178	0.038	−4.63	0.0001
	Al^{3+}	0.008	0.008	0.98	0.3294
TN90P	Soil pH	0.011	0.137	0.08	0.9346
	Al^{3+}	−0.062	0.030	−2.08	0.0403
TX10P	Soil pH	0.375	0.042	8.87	0.0001
	Al^{3+}	−0.012	0.009	−1.35	0.1799
TX90P	Soil pH	0.891	0.235	3.79	0.0003
	Al^{3+}	0.086	0.051	1.68	0.0973

Table 8
Estimated soil parameters under SSP2.6 under the extreme climate scenarios.

Predictors	Reponses	Estimate	Std Error	t Ratio	Sign
R95P	Soil pH	−0.02	0.020	−1.18	0.19
	Al^{3+}	0.002	0.001	3.44	0.001
R99P	Soil pH	−0.01	0.010	−1.66	0.101
	Al^{3+}	0.002	0.001	1.22	0.224
TN10P	Soil pH	−0.13	0.060	−2.10	0.040
	Al^{3+}	0.08	0.052	1.44	0.152
TN90P	Soil pH	0.50	0.230	2.23	0.029
	Al^{3+}	0.044	0.023	1.94	0.055
TX10P	Soil pH	0.32	0.071	4.48	0.0001
	Al^{3+}	−0.08	0.019	−4.07	0.0001
TX90P	Soil pH	0.22	0.074	3.13	0.0001
	Al^{3+}	−0.07	0.034	−2.07	0.0001

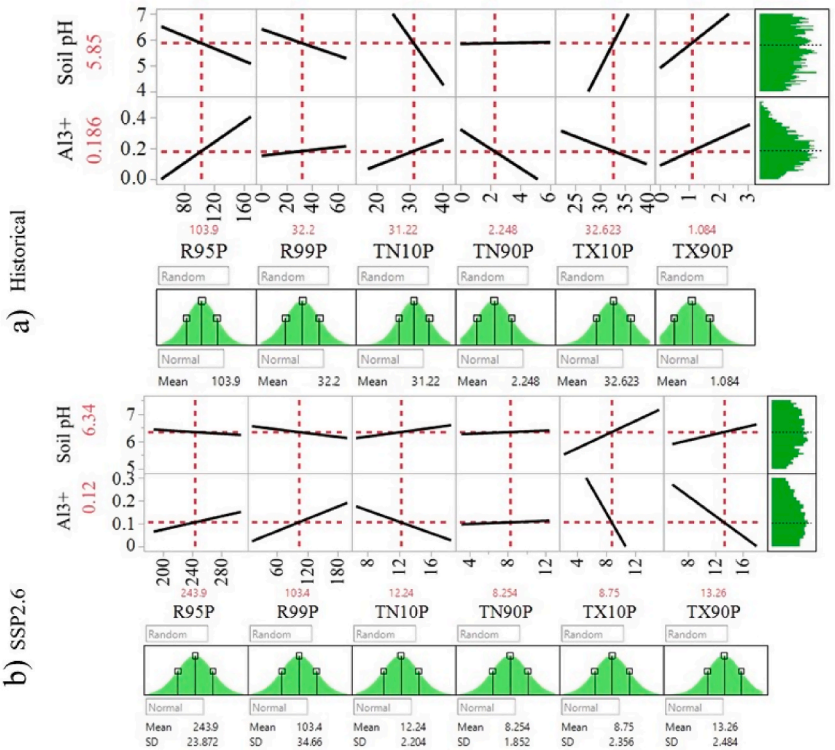

Fig. 4. The predicted profiles of soil pH and Al^{3+} in response to extreme climate indicators under the historical (a) and SSP2.6 (b) scenarios.

Table 9
Estimated soil parameters under the SSP4.5 extreme climate scenario.

Predictors	Responses	Estimate	Std Error	t Ratio	Sign
R95P	Soil pH	−0.01	0.006	−1.360	0.1768
	Al^{3+}	0.002	0.002	0.930	0.3535
R99P	Soil pH	−0.03	0.012	−2.410	0.0188
	Al^{3+}	0.002	0.004	0.670	0.5030
TN10P	Soil pH	−0.67	0.256	−2.640	0.0103
	Al^{3+}	0.10	0.079	1.290	0.2000
TN90P	Soil pH	−0.18	0.157	−1.170	0.2452
	Al^{3+}	0.01	0.048	0.290	0.7706
TX10P	Soil pH	1.3	0.109	11.910	0.0001
	Al^{3+}	−0.10	0.034	−2.870	0.0054
TX90P	Soil pH	0.38	0.146	2.580	0.0120
	Al^{3+}	−0.01	0.005	−2.237	0.0350

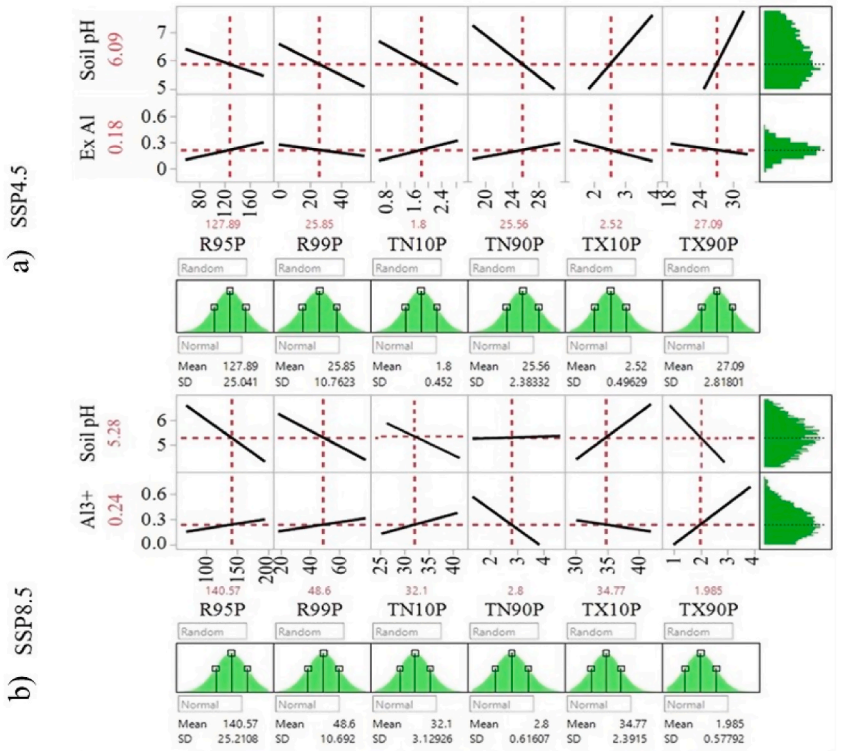

Fig. 5. Predictive profiles demonstrating the effects of extreme climate factors on the normal distribution of coffee tree soil parameters under the SSP4.5 (a) and SSP8.5 (b) scenarios.

Table 10
Estimated soil parameters under SSP8.5 extreme climate scenario.

Predictor	Responses	Estimate	Std Error	t Ratio	Sign
R95P	Soil pH	−0.018	0.0031	−5.75	0.0001
	Al^{3+}	0.001	0.0003	3.65	0.0004
R99P	Soil pH	−0.031	0.0069	−4.46	0.0001
	Al^{3+}	0.005	0.0015	3.09	0.0025
TN10P	Soil pH	−0.035	0.4042	0.09	0.9313
	Al^{3+}	0.016	0.0079	1.99	0.0496
TN90P	Soil pH	0.063	0.0220	2.84	0.0056
	Al^{3+}	−0.230	0.1449	−1.58	0.1165
TX10P	Soil pH	0.378	0.5052	0.75	0.4564
	Al^{3+}	−0.241	0.1811	−1.33	0.1869
TX90P	Soil pH	−0.186	0.0262	7.09	0.0001
	Al^{3+}	0.011	0.0094	1.20	0.2348

aluminum was predicted to increase significantly by 0.001, 0.005, and 0.016 % with increasing R95P, R99P, and TN10P, respectively.

3.2. Changes in soil pH and exchangeable aluminum under future climate scenarios

This study investigated the effects of projected changes in climate on soil pH and exchangeable aluminum levels. In this study, we examined the significant differences in climate change impacts on soil pH and exchangeable aluminum levels between different regions and different climate scenarios compared to those under historical climate conditions to understand the potential consequences for soil health and agricultural productivity. In Cluster-1, the model results indicate that the mean soil pH significantly decreased by 21.54 % under SSP8.5 but did not significantly change under the SSP4.5 and SSP8.5 scenarios compared to the historical soil conditions (Table 11). On the other hand, the exchangeable aluminum levels in Cluster-1 are projected to increase significantly under the SSP8.5 scenario by 581.82 %, while remaining relatively stable under the SSP2.6 and SSP8.5 scenarios. In cluster 2, the mean soil pH under the SSP2.6 and SSP4.5 scenarios will significantly increase by 13.29 and 7.87 %, respectively, but will continue to decrease by 7.51 % under the SSP8.5 scenario. Apparently, the exchangeable aluminum levels in cluster 2 are projected to decrease significantly under the SSP2.6 and SSP4.5 scenarios by 43.67 % and 17.47 %, respectively, but increase significantly by 18.34 % under the SSP8.5

scenario (Table 11).

Similarly, the soil pH and Al+3 concentration in Cluster 3 significantly differed under the different climate scenarios. The mean soil pH is projected to increase by 9.24 % under SSP2.6 and 4.39 % under SSP4.5 but decrease by 2.88 % under SSP8.5. The exchangeable aluminum levels in Cluster 3 are also projected to decrease by 24.9 % under the SSP2.6 scenario but will not significantly change under the SSP4.5 and SSP8.5 scenarios (Table 12). Overall, the model's diagnostic results under different climate scenarios reveal that climate change clearly affects soil health and agricultural productivity in the study area. Soil pH is generally expected to increase by 8.35 and 3.79 % under SSP2.6 and SSP4.5, respectively, but considerably decrease by 9.36 % under climate change scenarios. The Al^{3+} levels in the soil are also projected to decrease by 37.63 % under SSP2.6 but increase significantly by 45 % under SSP8.5.

In summary, this study revealed that climate change has a significant impact on soil health and agricultural productivity in the study area. The exchangeable aluminum levels and soil pH levels in Cluster-2 and Cluster-3 showed significant differences under the different climate scenarios. While soil pH levels are projected to increase under the SSP2.6 and SSP4.5 scenarios, they are expected to decrease under the SSP8.5 scenario. Similarly, the exchangeable aluminum levels in Cluster-2 are projected to decrease under the SSP2.6 and SSP4.5 scenarios but significantly increase under the SSP8.5 scenario. These findings highlight the importance of implementing climate change adaptation measures in agriculture to maintain soil health and productivity.

Fig. 6 illustrates the spatial impact of extreme climate indicators on soil pH under various scenarios. This study indicated that soil pH levels were lower in the northern and central parts of the region and higher in the eastern highlands of the Abbay basin under historical conditions. However, under the lower and intermediate emission scenarios (SSP2.6 and SSP4.5), the spatial distribution of soil pH is projected to change significantly. The western region is expected to experience a further decrease in soil pH due to the already acidic soil conditions. Conversely, the projected increase in alkaline soil conditions in the northern and central parts of the Abbay Basin ranged from 7 to 8.5 units. Under SSP8.5, the predicted changes in soil pH are expected to significantly decrease soil fertility and negatively affect crop productivity. The pH values of the western, central, and eastern regions of the basin are predicted to range from 4 to 5.5.

4. Discussion

The results indicate that the ANN model outperformed the multiple regression and bootstrapped fore models across several key performance metrics. Specifically, the ANN model achieved the highest accuracy and lowest mean squared error (MSE), demonstrating its superior ability to capture complex nonlinear relationships within the data. The superior performance of the ANN model can be attributed to its advanced structure, which allows for greater flexibility and learning capacity compared to traditional models [69]. This makes the ANN model a valuable tool for the predictive analysis of extreme climate influences on soil chemical reactions where precise and reliable predictions are essential.

The diagnostic findings of the model highlight the potential impacts of climate change on soil chemistry, specifically the decrease in soil pH and increase in the concentration of Al^{3+} ions under the SSP8.5 scenario. A decrease in soil pH and increase in aluminum ion concentration could have negative impacts on plant growth and ecosystem health. This study emphasizes the importance of considering multiple factors when analyzing the impact of climate change on soil by identifying predictors such as R95P, R99P, TX90P, and TN90P. An increase in R95P, R99P, and TN10P under the baseline conditions significantly decreased the soil pH but positively influenced the exchangeable Al^{3+} concentration. The increase in heavy precipitation and cold night temperatures might result in increased leaching of soil nutrients and decreased nutrient availability for plants. This could lead to reduced plant growth and productivity in the affected areas. Furthermore, the combination of heavy precipitation and cold temperatures might also increase the risk of soil erosion and runoff, which can further degrade soil quality and impact water quality in nearby streams and rivers.

On the other hand, the increase in TX10P and TX90P significantly improved the soil pH under the baseline conditions. This might promote microbial activity, increase the availability of nutrients in the soil and enhance the soil pH. Additionally, the increase in TX10P and TX90P may have reduced the leaching of acidic compounds, thereby reducing the acidity of the soil. Overall, these findings suggest that changes in TX10P and TX90P can play a crucial role in regulating soil pH and maintaining healthy soil chemistry and, ultimately, agricultural productivity. However, prolonged exposure of soil to high temperatures can also lead to soil moisture loss and increased erosion, which can ultimately negatively affect soil health. Previous studies have indicated that increasing temperatures can either cause soil acidification [70]or improve soil pH [71]. Other studies have indicated that heavy precipitation events can increase soil acidity and metal toxicity [72,73]. This study is also consistent with the findings of [8,74], and [75], who reported the impact of global climate change on soil health.

The positive impact of extreme climate indicators on soil pH indicates that reducing greenhouse gas emissions could decrease soil acidity. However, the negative impacts of R95P, R99P, and TN10P on soil pH and the positive impact on Al^{3+} ion concentration highlight the need for adaptation strategies to maintain soil health and promote plant growth. However, this can be seen in certain regions where heavy precipitation and cooling temperatures reduce soil pH, while warming temperatures actually improve soil pH and lead to increased crop productivity, such as in clusters 1 and 3. This highlights the need for localized research and management strategies, as the impacts of climate change on soil health can vary widely depending on specific conditions and ecosystems.

Moreover, this study highlights the complex interactions between climate change and soil chemistry and underscores the importance of continued research and monitoring to better understand and mitigate these impacts. It is also important for policymakers and researchers to consider these findings when developing strategies to mitigate the impacts of climate change on soil chemistry. This may include promoting practices that increase soil microbial activity and nutrient cycling, as well as reducing emissions that contribute to climate change [76,77]. Additionally, further research is needed to better understand the complex interactions between climate change and soil chemistry and to develop more effective strategies for mitigating these impacts. Overall,

Table 11
Soil pH changes under different climate change scenarios from 2015 to 2100.

Cluster	Scenarios	df	Mean	Difference	%	Std Error	t Ratio	Sign
1	Historical	29	6.44	–	–	–	–	–
	SSP2.6	29	6.47	0.03	0.47	0.15	0.18	0.855
	SSP4.5	29	6.22	−0.22	−3.40	0.15	−1.52	0.1387
	SSP8.5	29	5.10	−1.34	−21.54	0.15	−9.01	0.0001
2	Historical	44	5.72	–	–	–	–	–
	SSP2.6	44	6.48	0.76	13.29	0.12	6.19	0.0001
	SSP4.5	44	6.23	0.51	7.87	0.12	4.15	0.0002
	SSP8.5	44	5.19	−0.53	−8.51	0.12	−4.52	0.0001
3	Historical	53	5.63	–	–	–	–	–
	SSP2.6	53	6.15	0.52	9.24	0.06	8.69	0.0001
	SSP4.5	53	5.90	0.27	4.39	0.06	4.54	0.0001
	SSP8.5	53	5.46	−0.17	−2.88	0.08	−2.12	0.039
Overall	Historical	128	5.85	–	–	–	–	–
	SSP2.6	128	6.34	0.49	8.38	0.06	7.61	0.0001
	SSP4.5	128	6.09	0.24	3.79	0.06	3.73	0.0003
	SSP8.5	128	5.28	−0.57	−9.36	0.07	−7.62	0.0001

Table 12
Exchangeable Al changes under different climate change scenarios from 2015 to 2100.

Cluster	Scenarios	Df	Mean	Difference	%	Std Error	t Ratio	Sign
1	Historical	29	0.022	–	–	–	–	–
	SSP2.6	29	0.002	−0.020	−90.91	0.022	−1.06	0.2958
	SSP4.5	29	0.019	−0.003	−13.64	0.022	1.701	0.0997
	SSP8.5	29	0.15	0.128	581.82	0.02	6.293	0.0001
2	Historical	44	0.229	–	–	–	–	–
	SSP2.6	44	0.131	−0.10	−43.67	0.009	−10.9	0.0001
	SSP4.5	44	0.191	−0.04	−17.47	0.009	−4.22	0.0001
	SSP8.5	44	0.272	0.042	18.34	0.017	2.549	0.0144
3	Historical	53	0.241	–	–	–	–	–
	SSP2.6	53	0.177	−0.06	−24.90	0.01	−6.38	0.0001
	SSP4.5	53	0.237	−0.001	−0.41	0.01	−0.32	0.7493
	SSP8.5	53	0.263	0.022	9.13	0.014	1.59	0.1178
Overall	Historical	128	0.186	–	–	–	–	–
	SSP2.6	128	0.12	−0.07	−37.63	0.008	−8.69	0.0001
	SSP4.5	128	0.18	−0.01	−5.38	0.008	−0.79	0.431
	SSP8.5	128	0.24	0.054	45.00	0.01	5.321	0.0001

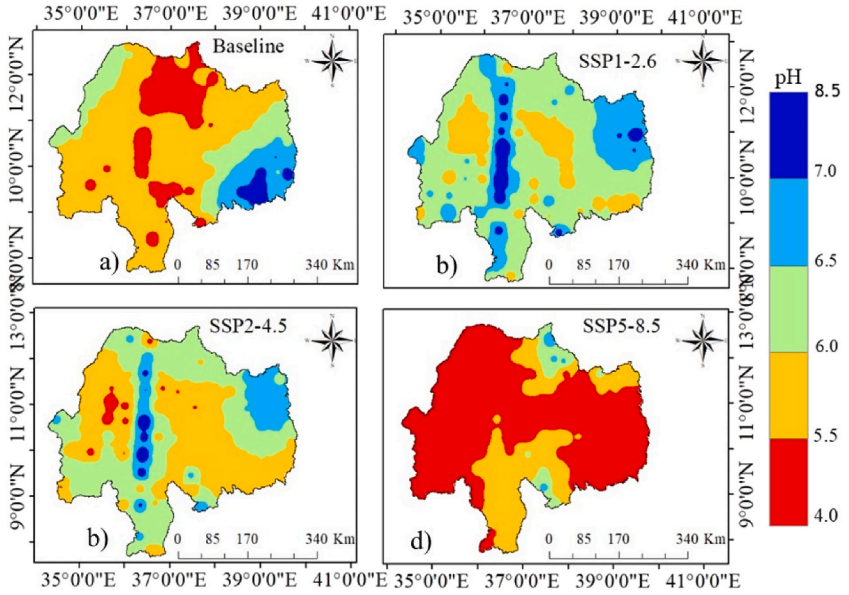

Fig. 6. The projected spatial changes in soil pH under baseline (a), SSP1-2.6 (b), SSP2-4.5 (c), and SSP5-8.5 (d) scenarios.

proactive measures are needed to protect soil health and promote sustainable ecosystem management in the face of climate change.

5. Strengths and limitations of the study

The study also highlighted the potential confounding variables that may have positive and negative influences on the results.

5.1. Strengths

- ✓ The use of advanced modeling techniques such as the neural network model enables precise and reliable predictions of soil acidity changes in response to extreme climate events.
- ✓ Focusing on the Abbay basin, a critical area for agriculture and water resources, makes the findings particularly relevant for local policy makers and stakeholders, aiding in better resource management and adaptation strategies.
- ✓ This study utilizes climatology, soil science, and environmental modeling to provide a comprehensive understanding of the relationships between climate extremes and soil properties.

5.2. Limitations

- ✓ The modeling approach, based on assumptions such as linearity and variable independence, may not fully capture the intricate interactions between climate indicators and soil acidity, potentially introducing biases in the results.
- ✓ The uncertainty of long-term climate projections could affect future soil acidity predictions, as models may not fully account for unexpected events or changes in land use patterns

6. Conclusion

This study highlights the significant impact of climate change on soil chemistry and agricultural productivity in the Abbay River Basin. The impacts of climate change on soil chemistry are complex and multifaceted, with both positive and negative effects on agricultural productivity. The impacts of extreme climate indicators on soil chemistry are complex and multifaceted, with both positive and negative effects on agricultural productivity. An increase in R95P, P99P and TX10P can also lead to increased soil acidity and toxicity, posing a threat to both crops and ecosystems. On the other hand, the increase in extreme climate indicators such as the TX10P and TX90P indicators will lead to an increase in soil pH and nutrient availability, which can have a positive impact on crop growth.

The projected changes in soil pH and exchangeable aluminum levels under the different climate scenarios varied from location to location. Soil pH levels are expected to increase under the SSP2.6 and SSP4 scenarios in the northern and central parts of the Abbay Basin but decrease under the SSP8.5 scenario across the region. The SSP2.6 and SSP4.5 scenarios predicted a decrease in exchangeable aluminum levels in Cluster 2, while the SSP8.5 scenario predicted a significant increase over the study area. These changes in soil pH and exchangeable aluminum levels can have significant impacts on agricultural productivity and nutrient availability in the Abbay Basin. An increase in soil pH can lead to improved nutrient uptake by plants, while a decrease can result in nutrient deficiencies. The anticipated increase in exchangeable aluminum levels under the SSP8.5 scenario could hinder crop growth by inhibiting root development and nutrient absorption. These findings highlight the importance of considering future climate scenarios when planning agricultural practices and soil management strategies in the region. The findings also emphasize the importance of implementing localized climate change adaptation measures in agriculture to maintain soil health and productivity, especially in areas that are vulnerable to the effects of climate change. It is crucial for farmers and policymakers to take proactive steps to mitigate the negative impacts of climate change on soil health and ensure sustainable agricultural practices for future generations.

Funding

None of the authors provided financial support for this research.

Data availability statement

The data that has been used is confidential.

CRediT authorship contribution statement

Fedhasa Benti Chalchissa: Writing – original draft, Visualization, Validation, Software, Project administration, Methodology, Investigation, Formal analysis, Data curation, Conceptualization. **Birhanu Kebede Kuris:** Writing – review & editing, Supervision, Resources.

Declaration of competing interest

The authors declare no conflicts of interest related to this study. All authors have completed the disclosure form for the Journal of Heliyon, and none of the relationships listed have influenced the study design, data collection, analysis, or interpretation of the results.

The funding sources had no role in the study design, data collection, analysis, interpretation of data, writing of the manuscript, or in the decision to submit the manuscript for publication. The authors declare that the research was conducted in the absence of any commercial or financial relationships that could be construed as a potential conflict of interest.

Acknowledgments

The primary authors are grateful for the opportunity to conduct this research and for the assistance provided by Wollega University. Without the support and resources provided by Wollega University, this study would not have been possible.

References

[1] M.M. Tahat, K.M. Alananbeh, Y.A. Othman, D.I. Leskovar, Soil health and sustainable agriculture, Sustain. Times 12 (12) (2020) 1–26.
[2] É. Dambrine, Soil acidity and acidification, Soils as a Key Compon Crit Zo 5 Degrad Rehabil 5 (2018) 83–95.
[3] European Soil Portal, Organic matter decline [Internet]. Fact Sheet No 3 - Org matter decline, 2009, https://esdac.jrc.ec.europa.eu/ESDB_Archive/eusoils_docs/other/eur23437.pdf (Assessed June 20, 2024).
[4] J.F. Ng, O.H. Ahmed, M.B. Jalloh, L. Omar, Y.M. Kwan, A.A. Musah, et al., Soil nutrient retention and pH buffering capacity are enhanced by calciprill and sodium silicate, Agronomy 12 (1) (2022) 1–24.
[5] C.O. Arévalo-Hernández, E. Arévalo-Gardini, A. Farfan, M. Amaringo-Gomez, A. Daymond, D. Zhang, et al., Growth and nutritional responses of juvenile wild and domesticated cacao genotypes to soil acidity, Agronomy 12 (12) (2022) 1–16.
[6] J. Fagúndez, X. Pontevedra-Pombal, Soil properties of North Iberian wet heathlands in relation to climate, management and plant community, Plant Soil [Internet] 475 (1–2) (2022) 565–580, https://doi.org/10.1007/s11104-022-05393-6.
[7] R. Ofoe, R.H. Thomas, S.K. Asiedu, G. Wang-Pruski, B. Fofana, Lord Abbey, Aluminum in plant: benefits, toxicity and tolerance mechanisms, Front. Plant Sci. 13 (January) (2023) 1–24.
[8] G. Gelybó, E. Tóth, C. Farkas, Kása I. Horel, Z. Bakacsi, Potential impacts of climate change on soil properties, Agrokem es Talajt 67 (1) (2018) 121–141.
[9] L. Zhang, Q. Zheng, Y. Liu, S. Liu, D. Yu, X. Shi, et al., Combined effects of temperature and precipitation on soil organic carbon changes in the uplands of eastern China, Geoderma 337 (November 2018) (2019) 1105–1115, https://doi.org/10.1016/j.geoderma.2018.11.026 [Internet].
[10] S. Cesco, T. Mimmo, G. Tonon, N. Tomasi, R. Pinton, R. Terzano, et al., Plant-borne flavonoids released into the rhizosphere: impact on soil bio-activities related to plant nutrition. A review [Internet], Biol. Fertil. Soils 48 (2) (2012 Feb 6) 123–149 [cited 2023 Jun 2], https://link.springer.com/article/10.1007/s00374-011-0653-2.
[11] V. Phogat, D. Mallants, J.W. Cox, J. Šimůnek, D.P. Oliver, J. Awad, Management of soil salinity associated with irrigation of protected crops, Agric. Water Manag. 227 (2020 Jan 20) 105845.
[12] M. Phour, S.S. Sindhu, Mitigating abiotic stress: microbiome engineering for improving agricultural production and environmental sustainability, Planta 256 (5) (2022) 1–34, 2565 [Internet]. 2022 Sep 20 [cited 2023 Jun 3], https://link.springer.com/article/10.1007/s00425-022-03997-x.
[13] A. Kumar, T. Bhattacharya, S. Mukherjee, B. Sarkar, A perspective on biochar for repairing damages in the soil–plant system caused by climate change-driven extreme weather events, Biochar 4 (1) (2022) 1–23, 41 [Internet]. 2022 Mar 24 [cited 2023 Jun 3], https://link.springer.com/article/10.1007/s42773-022-00148-z.
[14] L.T.T. Nguyen, Y. Osanai, I.C. Anderson, M.P. Bange, D.T. Tissue, B.K. Singh, Flooding and prolonged drought have differential legacy impacts on soil nitrogen cycling, microbial communities and plant productivity, Plant Soil 431 (1–2) (2018) 371–387.
[15] P.R. Kemp, J.M. Cornelius, J.F. Reynolds, A simple model for predicting soil temperatures in desert ecosystems, Soil Sci. 153 (4) (1992) 280–287.
[16] S. Reth, M. Reichstein, E. Falge, The effect of soil water content, soil temperature, soil pH-value and the root mass on soil CO2 efflux - a modified model, Plant Soil 268 (1) (2005 Jan) 21–33.
[17] E.A. Davidson, I.A. Janssens, Temperature sensitivity of soil carbon decomposition and feedbacks to climate change, Nature 440 (7081) (2006 Mar 9) 165–173.
[18] M. Bilgili, Prediction of soil temperature using regression and artificial neural network models, Meteorol. Atmos. Phys. 110 (1) (2010 Dec) 59–70.
[19] H. K, P. S, M. Manjunath, A. K Chakravarthy, Impact of climate change on soil health: emerging issues, Indian J. Appl. Res. 6 (3) (2023) 60–64.
[20] Y. Gong, P. Li, N. Sakagami, M. Komatsuzaki, No-tillage with rye cover crop can reduce net global warming potential and yield-scaled global warming potential in the long-term organic soybean field, Soil Tillage Res. 205 (2021 Jan 1) 104747.
[21] A. Beniaich, D.V. Guimarães, J.C. Avanzi, B.M. Silva, S.F. Acuña-Guzman, W.P. dos Santos, et al., Spontaneous vegetation as an alternative to cover crops in olive orchards reduces water erosion and improves soil physical properties under tropical conditions, Agric. Water Manag. 279 (2023 Apr 1) 108186.
[22] A. Amdihun, E. Gebremaria, L. Rebelo, G. Zeleke, Modeling soil erosion dynamics in the Blue Nile (Abbay) basin: a landscape approach, Res. J. Environ. Sci. 8 (5) (2014 May 1) 243–258.
[23] T. Molla, B. Sisheber, Estimating soil erosion risk and evaluating erosion control measures for soil conservation planning at Koga watershed in the highlands of Ethiopia, Solid Earth 8 (1) (2017 Jan 6) 13–25.
[24] B.G. Sinshaw, A.M. Belete, B.M. Mekonen, T.G. Wubetu, T.L. Anley, W.D. Alamneh, et al., Watershed-based soil erosion and sediment yield modeling in the Rib watershed of the Upper Blue Nile Basin, Ethiopia, Energy Nexus 3 (2021 Dec 15) 100023.
[25] T. Gomiero, Soil degradation, land scarcity and food security: reviewing a complex challenge, Sustain. Times 8 (3) (2016 Mar 18).
[26] S. Mesfin, G. Gebresamuel, M. Haile, A. Zenebe, Modelling spatial and temporal soil organic carbon dynamics under climate and land management change scenarios, northern Ethiopia, Eur. J. Soil Sci. 72 (3) (2021) 1298–1311.
[27] U.I. Udoumoh, A.F.A. Alonge, U.E. Ehiomogue, P. O, J.U. Okoko, I.I. Ahuchaogu, A review of the impacts of climate change on soil conditions and global food security, Iiard Int J Geogr Environ Manag. 9 (3) (2023) 43–58.
[28] H. k, P. S, M. Manjunath, A. K Chakravarthy, Impact of climate change on soil health: emerging issues, Indian J Appl Res 11 (13) (2023 Oct), 60-4, https://link.springer.com/article/10.1007/s12518-018-0249-8.
[29] M.A. Robi, A. Abebe, S.M. Pingale, Flood hazard mapping under a climate change scenario in a Ribb catchment of Blue Nile River basin, Ethiopia [Internet], Appl Geomatics 11 (2) (2019 Jun 1) 147–160 [cited 2023 Jun 3], https://link.springer.com/article/10.1007/s12518-018-0249-8.
[30] T.B. Tariku, T.Y. Gan, J. Li, X. Qin, Impact of climate change on hydrology and hydrologic extremes of upper Blue Nile River Basin, J Water Resour Plan Manag [Internet] 147 (2) (2020 Dec 3) 04020104 [cited 2023 Jun 3], https://ascelibrary.org/doi/abs/10.1061/%28ASCE%29WR.1943-5452.0001321.
[31] B. Getachew, B.R. Manjunatha, Potential climate change impact assessment on the hydrology of the lake Tana basin, upper Blue Nile River Basin, Ethiopia, Phys. Chem. Earth, Parts A/B/C 127 (2022 Oct 1) 103162.
[32] Gemada A. Regasa, Soil acidity challenges to crop production in Ethiopian highlands and management strategic options for mitigating soil acidity for enhancing crop productivity, Agric. For. Fish. 10 (6) (2021) 245. Available from: http://www.affjournal.com/Vol10No6/Soil-Acidity-Challenges-Ethiopian-Highlands.
[33] T. Belay, D.A. Mengistu, Impacts of land use/land cover and climate changes on soil erosion in Muga watershed, Upper Blue Nile basin (Abay), Ethiopia, Ecol Process [Internet] 10 (1) (2021), https://doi.org/10.1186/s13717-021-00339-9.
[34] Y.S. Kebede, N.T. Endalamaw, B.G. Sinshaw, H.B. Atinkut, Modeling soil erosion using RUSLE and GIS at watershed level in the upper beles, Ethiopia, Environ Challenges 2 (December) (2021) 100009, https://doi.org/10.1016/j.envc.2020.100009 [Internet].
[35] Y. Mohammed, F. Yimer, M. Tadesse, K. Tesfaye, Variability and trends of rainfall extreme events in north east highlands of Ethiopia, Int J Hydrol 2 (5) (2019). Available from: https://medcraveonline.com/IJH/IJH-02-00131.pdf.

[36] M. Bilgili, Ş. Ünal, A. Şekertekin, C. Gürlek, Machine learning approaches for one-day ahead soil temperature forecasting, Tarim Bilim Derg 29 (1) (2023 Jan 31) 221–238.
[37] A. Araghi, J. Adamowski, C.J. Martinez, J.E. Olesen, Projections of future soil temperature in northeast Iran, Geoderma 349 (2019 Sep 1) 11–24.
[38] M.S. Shiru, E.S. Chung, Performance evaluation of CMIP6 global climate models for selecting models for climate projection over Nigeria, Theor Appl Climatol [Internet] 146 (1–2) (2021) 599–615, https://doi.org/10.1007/s00704-021-03746-2.
[39] M. Meinshausen, Z.R.J. Nicholls, J. Lewis, M.J. Gidden, E. Vogel, M. Freund, et al., The shared socio-economic pathway (SSP) greenhouse gas concentrations and their extensions to 2500, Geosci. Model Dev. (GMD) 13 (8) (2020) 3571–3605.
[40] W.T. Hoyt, Z.E. Imel, F. Chan, Multiple regression and correlation techniques: recent controversies and best practices, Rehabil. Psychol. 53 (3) (2008) 321–339.
[41] G. Biau, E. Scornet, Rejoinder on: a random forest guided tour, Test 25 (2) (2016) 264–268.
[42] Y. Bengio, Deep learning deep learning, Nature 29 (7553) (2019) 1–73. Available from: https://www.nature.com/articles/s41586-019-1784-8.
[43] E. Teferi, S. Uhlenbrook, W. Bewket, Inter-annual and seasonal trends of vegetation condition in the Upper Blue Nile (Abay) Basin: dual-scale time series analysis, Earth Syst Dyn. 6 (2) (2015) 617–636.
[44] I. Tessema, B. Simane, Vulnerability analysis of smallholder farmers to climate variability and change: an agro-ecological system-based approach in the Fincha'a sub-basin of the upper Blue Nile Basin of Ethiopia, Ecol Process 8 (1) (2019).
[45] S. Tekleab, Y. Mohamed, S. Uhlenbrook, Hydro-climatic trends in the Abay/upper Blue Nile basin, Ethiopia, Phys. Chem. Earth, Parts A/B/C 61–62 (2013 Jan 1) 32–42.
[46] Mohammed J. Ali, T. Gashaw, G. Worku Tefera, Y.T. Dile, A.W. Worqlul, S. Addisu, Changes in observed rainfall and temperature extremes in the upper Blue Nile basin of Ethiopia, Weather Clim. Extrem. 37 (2022 Sep 1).
[47] T.H. Alemseged, R. Tom, Evaluation of regional climate model simulations of rainfall over the Upper Blue Nile basin, Atmos. Res. 161–162 (2015 Jul 1) 57–64.
[48] T. Hengl, G.B.M. Heuvelink, B. Kempen, J.G.B. Leenaars, M.G. Walsh, K.D. Shepherd, et al., Mapping soil properties of Africa at 250 m resolution: random forests significantly improve current predictions, PLoS One 10 (6) (2015) 1–26.
[49] E. Ribeiro, N.H. Batjes, J.G.B. Leenaars, A Van Oostrum, Jesus JM. De, Towards the standardization and harmonization of world soil data, in: Proced Man ISRIC World Soil Inf Serv (WoSIS Version 20), ISRIC World Soil Information, 2015, pp. 1–111 [Internet], https://www.isric.org/documents/towards-standardization-and-harmonization-world-soil-data.
[50] M. Nobakht, P. Beavis, S. O'Hara, R. Hutjes, I. Supit, Agroclimatic Indicators Product User Guide and Specification, ECMWF Copernicus, Bologna, Italy, 2019, https://doi.org/10.24381/5f47-a020.
[51] X. Hu, J.S. Næss, C.M. Iordan, B. Huang, W. Zhao, F. Cherubini, Recent global land cover dynamics and implications for soil erosion and carbon losses from deforestation, Anthropocene 34 (2021).
[52] H. Hersbach, B. Bell, P. Berrisford, S. Hirahara, A. Horányi, J. Muñoz-Sabater, et al., The ERA5 global reanalysis, Q. J. R. Meteorol. Soc. 146 (730) (2020 Jul 1) 1999–2049.
[53] M. Sadeghi, P. Nguyen, M.R. Naeini, K. Hsu, D. Braithwaite, S. Sorooshian, PERSIANN-CCS-CDR, a 3-hourly 0.04° global precipitation climate data record for heavy precipitation studies, Sci. Data 8 (1) (2021) 1–11.
[54] A.C. Cameron, F.A.G. Windmeijer, R-squared measures for count data regression models with applications to health-care utilization, J. Bus. Econ. Stat. 14 (2) (1996) 209–220.
[55] P.R. Jones, A note on detecting statistical outliers in psychophysical data, Atten. Percept. Psychophys. 81 (5) (2019) 1189–1196.
[56] A.S. Shirkhorshidi, S. Aghabozorgi, T.Y. Wah, T. Herawan, Big data clustering: a review. Lect Notes Comput Sci (including subser Lect Notes Artif Intell Lect Notes Bioinformatics) [Internet], LNCS 8583 (PART 5) (2014) 707–720 [cited 2023 Jun 6], https://link.springer.com/chapter/10.1007/978-3-319-09156-3_49.
[57] S. Zhu, D. Wang, T. Li, Data clustering with size constraints, Knowl. Base Syst. 23 (8) (2010 Dec 1) 883–889.
[58] L. Morissette, S. Chartier, The k -means clustering technique : general considerations and implementation in Mathematica 9 (1) (2013) 15–24.
[59] I.I. SAS, JMP 15 Predictive and Specialized Modeling, vol 516, 2020. https://www.amazon.com/JMP-Predictive-Specialized-Modeling-Second/dp/1629609641.
[60] N. Salkind, Honestly significant difference (HSD) test, Encycl Res Des. 1–5 (2012). https://www.utdallas.edu/~Herve/abdi-HSD2010-pretty.pdf.
[61] J.B. MacQueen, Some methods for classification and analysis of multivariate observations, in: Proceedings of the 5th Berkeley Symposium on Mathematical Statistics and Probability, Volume 1: Statistics, University of California Press, Berkeley, 1967, pp. 281–297. Available from: https://projecteuclid.org/euclid.bsmsp/1200512992.
[62] J. Wu, H. Xiong, J. Chen, Adapting the right measures for K-means clustering, in: Proc ACM SIGKDD Int Conf Knowl Discov Data Min, 2009, pp. 877–885.
[63] D. Berrar, Cross-validation, Encycl Bioinforma Comput Biol ABC Bioinforma 1–3 (April) (2018) 542–545.
[64] E. Danso-Amoako, T.D. Prasad, ANN model to predict the influence of chemical and biological parameters on Iron and Manganese accumulation, Procedia Eng [Internet] 70 (May) (2014) 409–418, https://doi.org/10.1016/j.proeng.2014.02.046.
[65] I.H. Sarker, Machine learning: algorithms, real-world applications and research directions, SN Comput Sci [Internet] 2 (3) (2021) 1–21, https://doi.org/10.1007/s42979-021-00592-x.
[66] M.A. Getahun, S.M. Shitote, Z.C. Abiero Gariy, Artificial neural network based modelling approach for strength prediction of concrete incorporating agricultural and construction wastes, Construct. Build. Mater. 190 (2018 Nov 30) 517–525.
[67] A. Pani, P.K. Sahu, F.A. Bhat, Assessing the spatial transferability of freight (trip) generation models across and within states of India: empirical evidence and implications for benefit transfer, Network. Spatial Econ. 21 (2) (2021) 465–493.
[68] F.B. Chalchissa, G.M. Diga, G.L. Feyisa, A.R. Tolossa, Impacts of extreme agroclimatic indicators on the performance of coffee (Coffea arabica L.) aboveground biomass in Jimma Zone, Ethiopia, Heliyon 8 (8) (2022) e10136, https://doi.org/10.1016/j.heliyon.2022.e10136 [Internet].
[69] M.S. Dantas, C. Christofaro, S.C. Oliveira, Artificial neural networks for performance prediction of full-scale wastewater treatment plants: a systematic review, Water Sci. Technol. 88 (6) (2023) 1447–1470.
[70] B. onwuka, B. Mang, Effects of soil temperature on some soil properties and plant growth [cited 2019 Dec 21]; Available from: http://medcraveonline.com, 2018.
[71] X. Guoju, Z. Qiang, B. Jiangtao, Z. Fengju, L. Chengke, The relationship between winter temperature rise and soil fertility properties, Air Soil. Water Res. 5 (2012) 15–22.
[72] A. McCauley, C. Jones, J. Jacobsen, Soil pH and organic matter, Nutr Manag Modul No 8 (8) (2009) 1–12 [Internet], https://citeseerx.ist.psu.edu/viewdoc/download?doi=10.1.1.566.6336&rep=rep1&type=pdf.
[73] C.A. Ditzler, A.J. Tugel, Soil quality field tools: experiences of USDA-NCRS soil quality institute, Agron. J. 94 (1) (2002) 33–38.
[74] A. P Mandal, S. Neenu, Impact of climate change on soil biodiversity-a review, Agric. Rev. 33 (4) (2012) 283–292.
[75] Y. Uwiragiye, Q.A.W. Khalaf, H.M. Ali, M.J.Y. Ngaba, M. Yang, A.S. Elrys, et al., Spatio-Temporal variations in soil pH and aluminum toxicity in sub-Saharan African croplands (1980–2050), Rem. Sens. 15 (5) (2023). https://www.mdpi.com/2072-4292/15/5/1338.
[76] K. Isobe, H. Oka, T. Watanabe, R. Tateno, R. Urakawa, C. Liang, et al., High soil microbial activity in the winter season enhances nitrogen cycling in a cool-temperate deciduous forest, Soil Biol. Biochem. 124 (2018 Sep 1) 90–100.
[77] J.W. Doran, E.T. Elliott, K. Paustian, Soil microbial activity, nitrogen cycling, and long-term changes in organic carbon pools as related to fallow tillage management, Soil Tillage Res. 49 (1–2) (1998 Nov 17) 3–18.